

Kinetic Investigation on Thermal Degradation of Empty Oil Palm Bunches Pyrolysis

Yeni Ria Wulandari^{1*}, Vinda Avri Sukma^{2,4}, Didik Supriadi³, Aulia Annas Mufti⁴, Yeni Variyana¹, Fadian Farisan Silmi¹, Adityas Agung Ramandani⁶, Sudibyo Sudibyo⁵, Ho Shing Wu⁶

¹ Department of Industrial Chemical Engineering Technology, Politeknik Negeri Lampung, Jl. Soekarno-Hatta 10, 35144 Rajabasa, Bandar Lampung, Indonesia

² Department of Environmental Engineering, Indonesia University, 16424 Pondok Cina, Depok City, West Java, Indonesia

³ Department of Chemical Engineering, Institute Teknologi Sumatera, Jl. Terusan Ryacudu, 35365 Way Huwi, Lampung, Indonesia

⁴ Department of Environmental Engineering, Institute Teknologi Sumatera, Jl. Terusan Ryacudu, 35365 Way Huwi, Lampung, Indonesia

⁵ Research Unit for Mineral Technology, Indonesia Institute of Sciences, Jl. Ir Sutami Km. 15, 35361 Tanjung Bintang, Lampung, Indonesia

⁶ Department of Chemical Engineering and Materials Science, Yuan Ze University, Yuan-Tung Road 135, 32003 Chung-Li, Taiwan

* Corresponding author, e-mail: yeniriawulandari@polinela.ac.id

Received: 31 August 2024, Accepted: 28 January 2025, Published online: 11 March 2025

Abstract

Empty oil palm bunches, a byproduct of the palm oil industry, are typically returned to plantations as mulch but represent a valuable renewable energy source. Through pyrolysis, these biomass residues can be converted into useful chemicals and energy. Before pyrolysis, the raw materials were characterized using thermogravimetric analysis (TGA), Fourier transform infrared spectroscopy (FTIR), and scanning electron microscopy with energy dispersive X-ray spectroscopy (SEM-EDX). Pyrolysis experiments were conducted on samples of 30, 60, and 80 mesh at temperatures of 350 °C, 450 °C, and 550 °C. TGA revealed a significant degradation peak at 301 °C, with kinetic analysis indicating a first-order reaction. Mineral analysis identified potassium as dominant, and SEM-EDX revealed a porous, fibrous structure in the bunches and the mineral with the highest content is potassium. The highest liquid yield of 38.76%, was achieved from the 80-mesh sample at 350 °C. Gas chromatography-mass spectrometry of the liquid fraction identified Vinyl methyl ether as the predominant compound, accounting for 96.81% of the composition.

Keywords

biomass energy, thermogravimetric analysis, bio-oil

1 Introduction

Indonesia is one of the largest producers of palm oil in the world. According to data from the Statistics Agency of Indonesia, the country produced 48.68 million tons of oil palm in 2022, which is used to generate crude palm oil.

The palm oil industry in Indonesia generates a significant amount of waste, including empty fruit bunches (EFBs), which account for about 23% of the total waste produced from processing fresh fruit bunches (FFBs). Despite their abundance, only around 10% of these EFBs are currently being utilized. This presents a significant opportunity to explore innovative ways to repurpose this waste material and reduce its environmental impact.

Furthermore, many Indonesian palm oil mills still use less sustainable methods for EFB disposal, such as incineration, open landfill, or using them as mulch or compost [1].

However, the incineration of empty oil palm bunches can contribute to air pollution and result in harmful emissions [2]. Converting biomass into bio-oil promotes a lignocellulosic biomass, primarily composed of cellulose, hemicellulose, and lignin, can be converted into bio-oil through pyrolysis [5]. The pyrolysis mechanism involves the thermochemical decomposition of hydrocarbon materials at high temperatures in the absence of oxygen. Cellulose, a polysaccharide composed of over 3,000 glucose units, has a degradation temperature of approximately 280–360 °C [6]. Hemicellulose is a heterogeneous polymer primarily utilized in bio-oil applications, exhibiting thermal degradation between 220 °C to 320 °C [7]. Lignin, a complex organic polymer, serves as a potential bio-oil source due to its aromatic structure [8]. Its decomposition

occurs primarily at temperatures ranging from 250 °C to 500 °C [9]. Pyrolysis generates several products, including bio-oil, charcoal, syngas, and other gaseous hydrocarbons [10, 11]. A recent study conducted by Wulandari et al. [12] reported that the pyrolysis of lignocellulosic biomass produces high-quality bio-oil and lignin at a temperature of 450 °C. Pyrolysis, a thermal degradation process, is a promising technique for converting oil palm waste, specifically EFBs, into valuable products. By heating EFBs in a batch reactor at 250–350 °C components like hemicellulose and cellulose degrade. This method offers advantages such as simple operation and low energy requirements, making it a potential solution for future energy needs. To explore this potential, researchers have conducted pyrolysis experiments on EFBs at 400 °C using a stainless steel reactor and 250–355 µm particle size [13]. The pyrolysis of empty oil palm fruit bunches at temperatures of 300 °C, 350 °C, and 400 °C yields the highest amount of bio-oil at 400 °C, while the optimal temperature for producing liquid smoke is 300 °C [14]. Additionally, catalytic pyrolysis of empty palm fruit bunches using a silica catalyst can produce a greater quantity of bio-oil products [15]. Kinetics in biomass pyrolysis can be calculated using thermogravimetric analysis (TGA) data. The Friedman iso-conversion method is a popular choice due to its simplicity and accuracy. However, its sensitivity to data noise can be mitigated through smoothing techniques, leading to more reliable results [16]. The iso-conversional method optimizes simulated data by varying activation energies and applying narrow conversion intervals, accurately calculating apparent activation energy (E_a) with minimal interference [17]. The Friedman method is a straightforward and widely utilized differential biomass conversion technique for kinetic analysis, particularly relevant for representing the pyrolysis process, and is commonly employed in kinetic studies [18].

2 Experimental

2.1 Materials

The raw material used consists of empty palm oil bunches collected from the Bekri palm oil processing facility in Lampung Province, Indonesia. These empty oil palm bunches are reduced in size to 30, 60, and 80 mesh and then dried in an oven at 105 °C for 12 h.

2.2 Pyrolysis process procedure

The pyrolysis process for empty oil palm fruit bunches were employed a batch reactor with a capacity of 4 L, which is equipped with a condenser. The pyrolysis is conducted at temperatures of 350, 450, and 550 °C. The process is considered

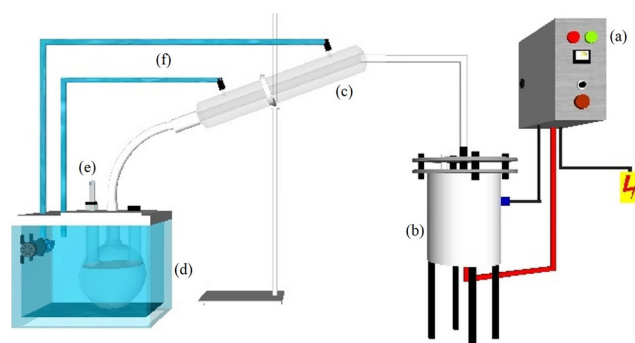


Fig. 1 Scheme of biomass pyrolysis process using batch reactor. (a) Control panel box, (b) reactor, (c) condenser, (d) cooling water, (e) product gas outlet pipe, (f) cooling water inlet and outlet flow

complete 2 h after no additional gas or bio-oil products are produced. This pyrolysis process was yielded bio-oil, char, and gas products. The bio-oil is obtained from the condensed gas and is stored in a three-neck flask connected to the condenser. Meanwhile, non-condensable gas exits the system, and the char produced during pyrolysis is collected after the process is complete and remains in the reactor. A schematic of the pyrolysis process in this study is shown in Fig. 1.

2.3 Analysis

The thermal analysis of the decomposition of empty oil palm fruit bunches was conducted using the Q50 Thermogravimetric Analyzer (TA Instruments, New Castle, Delaware, USA). The functional groups of the raw materials were analyzed by Fourier transform infrared spectroscopy (FTIR) using a Cary 630 FTIR Spectrometer (Agilent Technologies, Santa Clara, California, USA). The morphology and mineral elements present in the raw material of empty oil palm bunches were examined with field emission scanning electron microscopy coupled with energy dispersive X-ray spectroscopy (FESEM-EDX), (Quattro S Environmental SEM, Thermo Fisher Scientific, Waltham, Massachusetts, USA), by ASTM E986-97 standard [19]. The chemical composition of the bio-oil was analyzed using a GCMS-QP2010 SE (Shimadzu Corporation, Kyoto, Japan).

2.4 Study of kinetic on thermal degradation of raw material

Kinetics and E_a are critical factors to consider when designing a reactor. E_a can be determined using TGA data for the pyrolysis process [20]. To calculate the E_a in the biomass pyrolysis using TGA, researchers have employed the iso-conversional method, specifically the Friedman isoconversional method. This approach is widely used to illustrate the thermal degradation process of biomass due to its high accuracy and simplicity [16]. Kinetic calculations based on

TGA data for isothermal processes can be performed, Morin et al. [21] and E_α can be assessed at temperatures ranging from 150 to 700 °C using TGA data [12]. Isothermal degradation occurs at constant pressure and the rate of the degradation process is influenced by temperature (T) and the degree of conversion (α). The thermal degradation of biomass was determined using TGA method [12]. The degree of conversion can be derived from the mass loss during the degradation process (see Eq. (1)):

$$\alpha = \frac{m_0 - m_T}{m_0 - m_f}, \quad (1)$$

where m_0 denotes the initial mass, m_T represents the mass at a certain time, and m_f corresponds to the final mass.

The rate constant (k) is defined by the Arrhenius equation, as shown in Eq. (2):

$$k(T) = A e^{-\left(\frac{E_\alpha}{RT}\right)}, \quad (2)$$

where A is the pre-exponential factor or frequency factor (min^{-1}); E_α is the apparent activation energy of the decomposition reaction (kJ mol^{-1}); R is the universal gas constant ($8.314 \times 10^3 \text{ kJ mol}^{-1} \text{ K}^{-1}$); T is the absolute temperature (K).

The Friedman equation is expressed as follows [22], as illustrated in Eq. (3):

$$\ln\left(\frac{d\alpha}{dt}\right) = \ln[f(\alpha)A_\alpha] - \frac{E_\alpha}{RT}. \quad (3)$$

For illustrates the Friedman slope lines of $(\ln(d\alpha/dt)\alpha, i)$ versus $(1/T\alpha, i)$ during the conversion process from 0.1 to 0.9 for typical biomass degradation, as described in Eq. (4) [23]:

$$\ln\left(\frac{d\alpha}{dt}\right) = \ln f(\alpha) + \ln A_\alpha - \frac{E_\alpha}{RT}. \quad (4)$$

The degradation of biomass is a first-order reaction, represented by $f(\alpha)$ equal to $(1-\alpha)^n$, as shown in Eqs. (5) to (7):

$$\ln\left(\frac{d\alpha}{dt}\right) = \ln(1-\alpha)^n + \ln A_\alpha - \frac{E_\alpha}{RT}, \quad (5)$$

$$\ln\left(\frac{d\alpha}{dt}\right) - \ln(1-\alpha)^n = \ln A_\alpha - \frac{E_\alpha}{RT}, \quad (6)$$

$$\ln\frac{\frac{d\alpha}{dt}}{(1-\alpha)^n} = \ln A_\alpha - \frac{E_\alpha}{RT}. \quad (7)$$

If the degradation of lignin follows a first-order reaction, then $n = 1$ (Eqs. (8) and (9)):

$$\ln\frac{\frac{d\alpha}{dt}}{(1-\alpha)} = \ln A_\alpha - \frac{E_\alpha}{RT}. \quad (8)$$

$$\text{Hence, plot } \ln\frac{\frac{d\alpha}{dt}}{(1-\alpha)} \text{ vs } 1/T. \quad (9)$$

E_α is derived from the slope of its linear correlation with R and its value is calculated at each conversion degree [12]. Before reducing $d\alpha/dt$, data smoothing was performed due to the significant noise present in the data, which can affect the calculation of the E_α value. This process involves smoothing the data for the degree of conversion (α) and time (t) before deriving them, which is a crucial prerequisite for applying the Friedman method. Data smoothing can be achieved using MATLAB software [24] with the Savitzky–Golay filter; select a polynomial of degree 4 and a frame size of at least 10% of the total data or adjust it until the R^2 value on the graph approaches 1.

3 Result and discussion

3.1 Functional group analysis by FTIR

FTIR analysis was performed to identify the functional groups present in empty oil palm fruit bunches, as these groups are pertinent to the products generated from the pyrolysis process of the empty oil palm fruit bunches. The results of the FTIR analysis are shown in Fig. 2.

The FTIR results presented in Fig. 2 at a wavelength of 1018 cm^{-1} exhibit high intensity, indicating the presence of the C–O functional group, characteristic of alcohols and aliphatic ethers. The pronounced intensity of the C–O functional group is attributed to the deformation induced by secondary alcohols [25]. The carboxylic acid functional group, also characterized by high intensity, significantly influences the formation of acidic components [11]. Wavenumbers

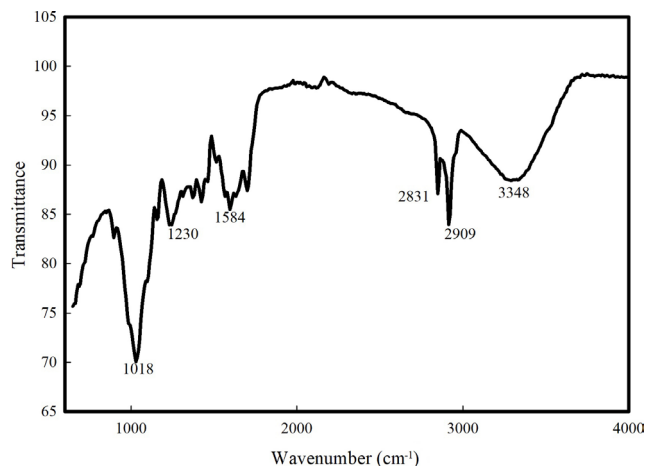


Fig. 2 FTIR analysis on empty palm oil bunches

1230 and 1584 cm^{-1} exhibit medium intensities corresponding to the functional groups C=O and C=C, respectively [26]. The C=O functional group is associated with condensed guaiacyl (G) units, where G serves as a monomer of lignin. The lignin content in empty oil palm fruit bunches is reported to be 17% [27]. In other studies, the lignin content in empty oil palm fruit bunches was found to be 18% [28], which influences the intensity of the C=O functional group. The C=O functional group can produce aromatic components. Wavenumbers 1593, 1506, and 1457 cm^{-1} correspond to the deformation of lignin aromatic rings [26]. Wavenumber 2831 cm^{-1} exhibits medium intensity, while wavenumbers 2909 cm^{-1} and 3348 cm^{-1} demonstrate high intensity. Wavenumbers 2831 cm^{-1} and 2909 cm^{-1} correspond to the C–H functional groups. The range of wavenumbers from 2985 cm^{-1} to 2336 cm^{-1} represents the C–H stretching vibrations of the methyl and methylene groups [26]. It is well established that the peak between 2900 cm^{-1} and 1700 cm^{-1} , corresponding to C–H bonds, indicates the presence of hemicellulose in empty oil palm fruit bunches [29]. At a peak wavenumber of 3348 cm^{-1} , the O–H functional group exhibits stretching due to the presence of alcohol. Additionally, another research indicates that for empty oil palm fruit bunches, a wavenumbers of 3355 cm^{-1} corresponds to the stretching of O–H bonds [30].

3.2 Thermogravimetric analysis (TGA) and kinetic calculations

The TGA and differential thermogravimetric (DTG) graphs span a temperature range of 100 to 700 °C, as illustrated in Fig. 3, which is divided into three distinct stages. In stage 1, within the temperature range of 100–200 °C, there is a mass reduction of only 2%. During this phase, the moisture content in empty oil palm bunches is eliminated. The TGA analysis of biomass in stage 1 focuses on

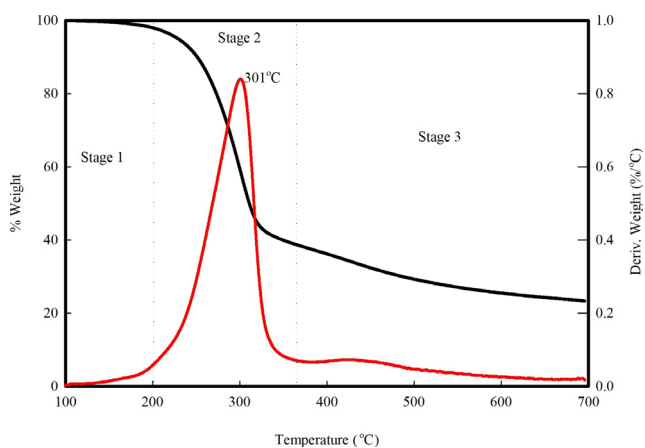


Fig. 3 TGA and DTG graphs of empty oil palm bunches

the removal of moisture from the material [12]. In the temperature range of 200 to 370 °C, the most significant mass loss occurs, primarily due to the degradation of hemicellulose, cellulose, and a small amount of lignin. The main peak at 301 °C indicates the degradation of cellulose [31]. Cellulose is the predominant component of biomass, which explains why the highest peak occurs in stage 2. The third stage degrades lignin and any remaining unbroken cellulose. However, during this stage, char formation also takes place [32]. Based on the TGA data presented, the E_{α} is calculated using Eqs. (7) and (8), and the results are plotted according to Eq. (9). The outcomes of the E_{α} calculations are illustrated in Fig. 3. $E_{\alpha 0}$ is derived directly from Eq. (8) and is subsequently used in Eq. (9). In contrast, $E_{\alpha 1}$ is calculated using Eq. (7), where the value n is set to 1. The n value in Eq. (7) represents the reaction order in the pyrolysis process. A first-order reaction is typically employed to calculate the reaction kinetics in biomass pyrolysis [33]. It can be observed in Fig. 4 that the graphs of $E_{\alpha 0}$ and $E_{\alpha 1}$ exhibit different values, yet the patterns are nearly identical. The first reaction order demonstrates a more optimal value for modeling biomass pyrolysis [34]. The degree of conversion ranges from 0.01 to 0.9. Within the range of 0.001 to 0.3, the E_{α} values range from 113 to 137 kJ mol^{-1} . During this phase, the cracking of the carbon bonds in empty oil palm fruit bunches occurs, leading to the degradation of cellulose and hemicellulose. At conversion levels of 0.4 and 0.5, the E_{α} values decrease to 77 and 83 kJ mol^{-1} , respectively. Subsequently, there is an increase in E_{α} at conversion levels of 0.7 and 0.8, with values of 210 and 338 kJ mol^{-1} . The increase signals lignin degradation, requiring greater energy for breakdown. At a conversion level of 0.9, there is a decrease in E_{α} due to the onset of char formation.

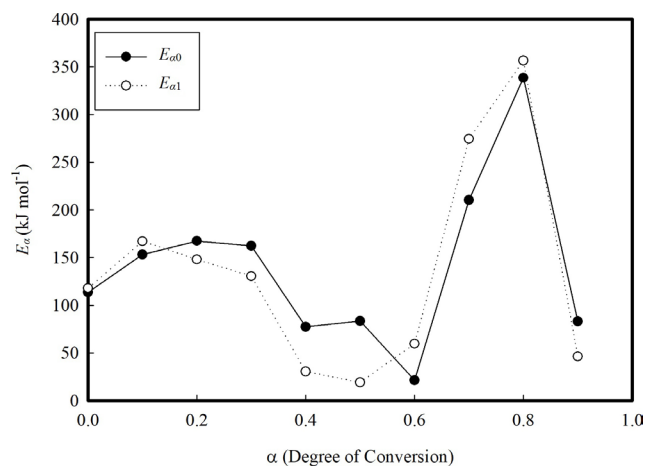


Fig. 4 E_{α} from pyrolysis of empty oil palm fruit bunches based on TGA data

The results presented in Table 1 are derived using Eq. (7), where the reaction rate, da/dt , is calculated as the product of the rate coefficient k and the conversion function $f(\alpha)$, based on first-order kinetics [34]. A , determined using the Friedman method, varies from a conversion degree of 0.0 to 0.9, depending on the value E_a . The values of A and E_a are inversely proportional. This E_a value fluctuates, indicating and predicting the degradation of lignocellulose. The E_a required for the degradation of cellulose and hemicellulose is lower than that required for lignin degradation. The DTG curve can reveal variations in the lignocellulosic composition present in biomass. In the DTG curve presented in this research, a prominent peak is observed at a temperature of 301 °C (see Fig. 3), which corresponds to the degradation of the holocellulose component. This degradation occurs at a conversion degree of 0.0 to 0.3, within a temperature range of 150 °C to 320 °C, with an E_a value ranging from 117 to 147 kJ mol⁻¹. Conversely, temperatures below 150 °C, which pertain to the removal of water content from the biomass in this study, are not included in the calculation of reaction kinetics. Degree of conversion 0.0 is the beginning of hemicellulose degradation with a total E_a of 117 kJ mol⁻¹ which occurs at a temperature range of 150–244 °C in TGA data. At degree of conversion 0.1 with a temperature range in TGA of 245–265 °C with a total E_a of 166.99 kJ mol⁻¹, hemicellulose and cellulose degradation occurs. Hemicellulose is the most easily degraded lignocellulose, followed by cellulose. However, at degree of conversion 0.2–0.3 with a temperature range of 266–288 °C cellulose degradation occurs. Degree of conversion 0.4–0.6 with a TGA temperature of 289–2316 °C experienced a decrease in total E_a to 30.33–59.64 kJ mol⁻¹, where at that point the peak of the greatest mass loss occurred. Empty oil palm bunches contain cellulose. In this condition indicates that cellulose degradation has been completed. Degree of conversion 0.7–0.8

experienced an increase in total E_a to 274.37 kJ mol⁻¹ and 356.44 kJ mol⁻¹ in the TGA temperature range of 317–470 °C, where at that time cellulose degradation occurred and lignin degradation began. Lignin components are the most difficult to degrade and require high temperatures. The last degree of conversion 0.9 is the formation of char and the lignin degradation process has been completed which occur at a temperature of 471–695 °C.

The thermal degradation of empty oil palm fruit bunches is characterized by the formation of complex components in the first reaction order, involving multiple highly reactive phases over a short duration [35]. The high levels of hemicellulose and cellulose in empty palm fruit bunches significantly contribute to the weight removal process during stage 2. This results in visible peaks on the DTG graph, particularly at a degree of conversion ranging from 0.0 to 0.7, which corresponds to the volatile components present in the empty palm fruit bunches [36]. The elevated levels of volatile matter and fixed carbon contribute to the significant presence of condensable and non-condensable chemical compounds in empty oil palm fruit bunches, which can impact the product during pyrolysis [35]. The final weight percentage in stage 2 is 40%, indicating that the volatile components present in empty oil palm bunches account for 58%. The highest E_a occurs at a conversion degree of 0.8, within a temperature range of 367 to 470 °C, where lignin degradation takes place. At a conversion degree of 0.9 and 470 °C, the process shifts towards char formation. During this phase, carbon, hydrogen, and oxygen elements break down, yielding new elements and leaving only carbon and mineral residues to form char. This final stage does not require a high energy input, as it has an E_a of 46 kJ mol⁻¹ and signifies the transition to the third stage. The char produced at the end of this process is referred to as fixed carbon. TGA indicates that 25% of the final weight of thermally degraded empty oil palm bunches is fixed carbon, primarily derived from lignin. This fixed carbon measurement can be used to predict char yield during pyrolysis.

Table 1 Kinetic parameter of empty fruit bunch pyrolysis on first-order

α	R^2	k	E_{a1} (kJ mol ⁻¹)	A (s ⁻¹)
0.00	0.98	0.0015	117.79	1.025×10^{-9}
0.10	0.99	0.0375	166.99	7.093×10^{-11}
0.20	0.99	0.0812	147.92	1.523×10^{-9}
0.30	0.99	0.1256	130.46	1.923×10^{-8}
0.40	1.00	0.1793	30.33	4.670×10^{-3}
0.50	0.99	0.2388	19.07	2.408×10^{-2}
0.60	0.99	0.2882	59.64	2.208×10^{-4}
0.70	1.00	0.2198	274.37	1.023×10^{-15}
0.80	0.99	0.0521	356.44	1.253×10^{-20}
0.90	0.99	0.0801	46.12	3.120×10^{-4}

3.3 Morphological and elemental analysis

The morphology of empty palm oil bunches is illustrated in Fig. 5 The first image on the left displays a magnification of 1000×, the second image on the right shows a magnification of 2500× and the third image at the bottom is a magnification of 5000×. This image demonstrates the fiber richness of empty palm oil bunches. A closer examination of the lower image indicates that these bunches possess a porous

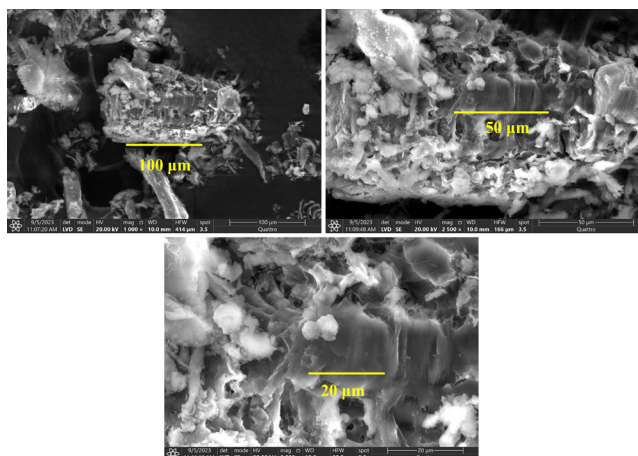


Fig. 5 Morphology of oil palm empty bunches

structure. Consequently, in Indonesia, empty palm oil bunches from factories are returned to plantation land to be used as mulch. Due to their porous nature, the decomposition process occurs more rapidly. The surface of empty palm oil bunches resembles fibrous material, characterized by numerous pores and a rigid texture [37]. Additionally, the surface of empty oil palm bunches is coated with wax and impurities, with the entire surface covered in lignin and a waxy layer [38]. An elemental analysis of empty oil palm bunches is presented in Table 2.

Table 2 highlights the predominant carbon and oxygen components, which are the primary organic constituents found in biomass. The main organic components of biomass are carbon, hydrogen, and oxygen. These elements are interconnected to form long chains, influencing the pyrolysis products generated from the cleavage of organic carbon bonds. The carbon content in empty oil palm bunches has been reported to be 47.08% and 50.24% (48.66 ± 1.58), while previous studies indicated oxygen content levels of 42.57% and 36.03% [39, 40]. The inorganic components in empty oil palm bunches consist of minerals influenced by the ecosystem where oil palm plants grow and by the plants inherent characteristics. The minerals present in oil palm

Table 2 Elements contained in empty oil palm fruit bunches

Element	Mass (%)
Carbon	58.97
Oxygen	39.7
Potassium	6.59
Aluminum	1.74
Magnesium	1.13
Calcium	0.5
Sulfur	0.29
Chlorine	0.26
Silicon	0.12

include potassium, aluminum, magnesium, calcium, sulfur, chlorine, and silicon. Potassium is the most abundant mineral in empty oil palm bunches, comprising 48.94 wt% of the ash content [41]. Due to their high potassium content, empty oil palm bunches are an excellent choice for use as fertilizer. In Indonesia, these empty oil palm bunches are typically returned to the plantation after the pressing process, allowing them to serve as mulch and natural fertilizer. However, when used as fuel, the high mineral content can lead to the formation of crusts, which may inhibit energy conversion efficiency. Additionally, minerals can create issues during the combustion process in the furnace, resulting in suboptimal heating performance [42].

3.4 Pyrolysis product yields and characteristics

Fig. 6 illustrates the results of pyrolysis conducted on empty oil palm bunches, varying in size and temperature. For bio-oil products derived from particle sizes of 30, 60, and 80 mesh, no significant differences were observed. However, the gas and solid products were influenced by the size of the raw material. At a particle size of 30 mesh, an increase in pyrolysis temperature resulted in a significant rise in gas production, while the solid product experienced a notable decrease. In contrast, for smaller particle sizes of 60 mesh and 80 mesh, an increase in temperature led to an insignificant rise in gas production, with a similar trend observed for solid products. Essentially, empty oil palm bunches resemble fibers; samples sized at 30 mesh are more voluminous and hollow compared to those sized at 60 mesh and 80 mesh. Due to their hollow structure, combustion during the pyrolysis process is more uniform, resulting in a higher yield of gas products at elevated

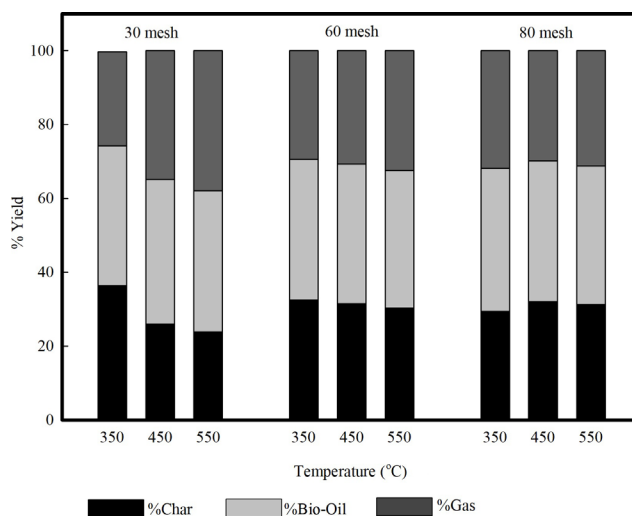


Fig. 6 Yield of pyrolysis products with variations in temperature and particle size

temperatures. Conversely, the 60 mesh and 80 mesh sizes are denser, causing heat to be transferred from the reactor wall to the sample particles and subsequently to adjacent particles. The difference in sample sizes between 60 mesh and 80 mesh showed no significant variation in results.

Moreover, the pyrolysis products are also influenced by the heating rate of the reactor. Consequently, the volume of bio-oil obtained is affected by variations in size and temperature during pyrolysis. As the pyrolysis temperature increases, the yield of gas products surpasses that of liquid products. Conversely, if the temperature is too low, the primary product generated will be charcoal [12]. The initial pyrolysis of empty oil palm bunch degradation occurs at a temperature of 117 °C, at which point smoke begins to emerge from the condenser. The second degradation phase occurs at a temperature of 193 °C, resulting in bio-oil being released from the condenser into the boiling flask. In Fig. 3, the TGA indicates that degradation commences at 114 °C, marking the onset of weight loss in the sample. The sample subsequently undergoes its first peak weight loss at 319 °C, where each component decomposes into char, bio-oil, and gas. The degradation profiles observed in TGA and pyrolysis exhibit no substantial differences. Similarly, the char products from both pyrolysis and TGA display comparable final results. The char produced at an 80 mesh size at 550 °C yields 37%, while TGA results in a char yield of 35%. This suggests that the degradation temperatures in pyrolysis and TGA are quite similar. The bio-oil obtained displays two distinct phases: a black phase and a brownish-yellow phase, both of which emit a sharp odor. Furthermore, the charcoal product is characterized by its black color.

A burn test was conducted to assess the combustibility of the bio-oil. Samples of 80 mesh at 350 °C and 440 °C, and 60 mesh at 350 °C and 450 °C were tested, as these produced the black phase of bio-oil. The test involved dipping a wick into the bio-oil and igniting it. Only the black phase was combustible, while the brownish-yellow phase could not be ignited. The black phase is less dense than the brownish-yellow phase, remaining separated and floating above the yellow phase when combined. The brownish-yellow phase likely contains a higher moisture content, which prevents it from igniting during the test. The burn test results indicate that the black phase bio-oil can sustain a flame for 33 s. However, the liquid product obtained from the pyrolysis of empty oil palm bunches cannot be directly used as a fuel source. A series of additional processes must be implemented to convert it into



Fig. 7 Burn test on black phase bio-oil product

biofuel. Fig. 7 illustrates the results of the burn test on bio-oil. Biomass pyrolysis produces bio-oil, which is divided into two phases: a water-rich phase (over 90% water) and an oil phase with significantly lower water content.

The principle of pyrolysis in this study is slow pyrolysis. In slow pyrolysis, the char product becomes the product with the highest yield. This high-yield char product can be used as bio-briquettes, serving as a renewable solid fuel. Additionally, char can be developed into activated carbon, soil ameliorants, and supercapacitors. In the pyrolysis process, the sought-after product is bio-oil, which holds promise as a renewable liquid fuel. To reduce char products and increase bio-oil production, techniques such as using catalysts, co-pyrolysis, inert gases like nitrogen, and switching to fast pyrolysis can be employed. Slow pyrolysis is energy-intensive and may not be comparable to the value of its products. As a result, future pyrolysis processes may utilize innovative technologies like microwave-assisted pyrolysis.

3.5 GC-MS analysis of bio-oil

The bio-oil obtained from the pyrolysis of empty oil palm bunches consists of two distinct phases: a black upper phase and a brownish-yellow lower phase. Each phase was analyzed separately using GC-MS, with the sample being 80-mesh size at a temperature of 350 °C. Table 3 summarizes the GC-MS analysis of pyrolysis products in the black phase, listing the area percentages, molecular formulas, and associated chemical components.

The dominant compound, representing 96.81% of the area, is vinyl methyl ether (C_3H_6O), which indicates that this ether is the primary product formed during the pyrolysis process in this phase. Following vinyl methyl ether, the second highest component is benzene (C_6H_6), which accounts for 1.27%, indicating the presence of

Table 3 GC-MS compound components of pyrolysis products in the black phase

Area (%)	Molecular formula	Component
96.81	C ₃ H ₆ O	Vinyl methyl ether
0.67	C ₆ H ₁₄	Butane
0.47	C ₆ H ₁₂	Cyclopentane
0.43	C ₆ H ₁₂ O ₆	Hexane
1.27	C ₆ H ₆	Benzene
0.18	C ₇ H ₁₄	1-Heptene
0.14	C ₇ H ₁₄	Cyclopentane

aromatic hydrocarbons. Other components are present in much smaller amounts: butane (C₆H₁₄) at 0.67%, cyclopentane (C₆H₁₂) at 0.47%, and hexane (C₆H₁₂O₆) at 0.43%. Additionally, 1-heptene (C₇H₁₄) is found at 0.18%, and cyclopentane (C₇H₁₄) at 0.14%, further contributing to the hydrocarbon mix in this phase.

Additionally, Table 4 presents the GC-MS analysis results of the pyrolysis products in the yellow phase, showing the area percentages of various compounds along with their molecular formulas. The most dominant component, with an area percentage of 54.48%, is acetic acid (C₂H₄O₂), which is also observed in a smaller amount at 9.67%. This suggests that acetic acid is a major product of the pyrolysis process. The second largest component, representing 18.47% of the area, is 2-propanone (C₃H₆O), a type of ketone. Following that, phenol (C₆H₆O) accounts for 10.95%, indicating the presence of aromatic compounds. Furthermore, other minor components include 2-furanmethanol (C₅H₁₀O₂) at 1.51%, 2(3H)-furanone (C₄H₆O₂) at 1.03%, cyclooctane (C₈H₁₆) at 1.35%, and 2-methylphenol (C₇H₈O) at 1.27%. Lower percentages indicate

Table 4 GC-MS Compound components of pyrolysis products in the yellow phase

Area (%)	Molecular formula	Component
18.47	C ₃ H ₆ O	2-propanone
54.48	C ₂ H ₄ O ₂	Acetic acid
9.67	C ₂ H ₄ O ₂	Acetic acid
1.51	C ₅ H ₁₀ O ₂	2-Furanmethanol
1.03	C ₄ H ₆ O ₂	2(3H)-Furanone
10.95	C ₆ H ₆ O	Phenol
1.35	C ₈ H ₁₆	Cyclooctane
1.27	C ₇ H ₈ O	Phenol, 2-methyl

the presence of furan and other cyclic compounds, which are less prevalent than acetic acid and phenol derivatives. The composition of the bio-oil components is influenced by the conditions and raw materials used during pyrolysis [11].

Pyrolysis of EFBs at a temperature of 390 °C yields various organic compounds, with phenolic compounds as the primary component, followed by ketones, other aromatic compounds (compounds containing benzene), alcohols, and esters [28]. The role of biomass regarding recent advances in technology. Microwave pretreatment is a promising technique to enhance the bioconversion of lignocellulosic biomass to biofuels. By disrupting the biomass structure, it increases the accessibility of cellulose and hemicellulose to enzymes, resulting in higher sugar yields and improved biofuel production [43]. Acid-based biorefineries use acid hydrolysis to break down lignocellulosic biomass into simple sugars, which can be fermented into biofuels like ethanol [44]. Steam explosion (SE) is a pretreatment method that disrupts biomass structure, increasing porosity and enzyme accessibility for hydrolysis. It's effective in releasing hemicellulose sugars, making it valuable in biorefineries [45]. All three of these pretreatment methods share a common goal to unlock the potential of lignocellulosic biomass as a renewable resource for biofuel production. By breaking down the complex structure of biomass and increasing the accessibility of its constituent sugars, these techniques contribute to a more sustainable and environmentally friendly energy future.

4 Conclusion

Empty oil palm bunch waste can be converted into bio-oil through pyrolysis. However, combustion tests indicate that the bio-oil, particularly the black phase, requires further processing to be a suitable biofuel. TGA analysis reveals three main degradation phases: moisture removal, lignocellulose decomposition, and char formation. The high potassium content of the char makes it a potential fertilizer. Particle size and temperature influence pyrolysis product yields, with larger particles favoring gas production at higher temperatures. GC-MS analysis showed distinct phases in the bio-oil, with vinyl methyl ether dominating the black phase and acetic acid the yellow phase. While the black phase is more combustible, both phases necessitate further refinement for commercial fuel use.

References

- [1] Hau, L. J., Shamsuddin, R., May, A. K. A., Saenong, A., Lazim, A. M., Narasimha, M., Low, A. "Mixed Composting of Palm Oil Empty Fruit Bunch (EFB) and Palm Oil Mill Effluent (POME) with Various Organics: An Analysis on Final Macronutrient Content and Physical Properties", *Waste and Biomass Valorization*, 11(10), pp. 5539–5548, 2020.
<https://doi.org/10.1007/s12649-020-00993-8>
- [2] Lee, S. Y., Alam, T., Kim, J.-H., Lee, J.-C., Park, S.-W. "Qualitative analysis of tar based on tar sampling conditions for empty fruit bunch gasification", *Biomass Conversion and Biorefinery*, 13(6), pp. 4695–4704, 2023.
<https://doi.org/10.1007/s13399-021-01567-x>
- [3] Chen, W., Lei, Y. "The impacts of renewable energy and technological innovation on environment-energy-growth nexus: New evidence from a panel quantile regression", *Renewable Energy*, 123, pp. 1–14, 2018.
<https://doi.org/10.1016/j.renene.2018.02.026>
- [4] Detchusananard, T., Wuttipisan, N., Limleamthong, P., Prasertcharoensuk, P., Maréchal, F., Arpornwichanop, A. "Pyrolysis and gasification integrated process of empty fruit bunch for multi-biofuels production: Technical and economic analyses", *Energy Conversion and Management*, 258, 115465, 2022.
<https://doi.org/10.1016/j.enconman.2022.115465>
- [5] Prashanth, P. F., Kumar, M. M., Vinu, R. "Analytical and microwave pyrolysis of empty oil palm fruit bunch: Kinetics and product characterization", *Bioresource Technology*, 310, 123394, 2020.
<https://doi.org/10.1016/j.biortech.2020.123394>
- [6] Stefanidis, S. D., Kalogiannis, K. G., Iliopoulou, E. F., Michailof, C. M., Pilavachi, P. A., Lappas, A. A. "A study of lignocellulosic biomass pyrolysis via the pyrolysis of cellulose, hemicellulose and lignin", *Journal of Analytical and Applied Pyrolysis*, 105, pp. 143–150, 2014.
<https://doi.org/10.1016/j.jaap.2013.10.013>
- [7] Wang, J., Minami, E., Asmadi, M., Kawamoto, H. "Thermal degradation of hemicellulose and cellulose in ball-milled cedar and beech wood", *Journal of Wood Science*, 67(1), 32, 2021.
<https://doi.org/10.1186/s10086-021-01962-y>
- [8] Wang, J., Liu, Z., Li, J., Yan, B., Tao, J., Cheng, Z., Chen, G. "In-situ hydrodeoxygenation of lignin via hydrothermal liquefaction with water splitting metals: comparison between autocatalytic and non-autocatalytic processes", *International Journal of Hydrogen Energy*, 47(11), pp. 7252–7262, 2022.
<https://doi.org/10.1016/j.ijhydene.2021.12.086>
- [9] Yang, H., Gong, M., Hu, J., Liu, B., Chen, Y., Xiao, J., Li, S., Dong, Z., Chen, H. "Cellulose Pyrolysis Mechanism Based on Functional Group Evolutions by Two-Dimensional Perturbation Correlation Infrared Spectroscopy", *Energy & Fuels*, 34(3), pp. 3412–3421, 2020.
<https://doi.org/10.1021/acs.energyfuels.0c00134>
- [10] Saghir, M., Zafar, S., Tahir, A., Ouadi, M., Siddique, B., Hornung, A. "Unlocking the Potential of Biomass Energy in Pakistan", *Frontiers in Energy Research*, 7, 24, 2019.
<https://doi.org/10.3389/fenrg.2019.00024>
- [11] Wulandari, Y. R., Silmi, F. F., Ermaya, D., Sari, N. P., Teguh, D. "Efek Suhu Pirolisis Jerami Padi Untuk Produksi Bio-Oil Menggunakan Reaktor Batch" (Effect of Rice Straw Pyrolysis Temperature for Bio-Oil Production Using a Batch Reactor), *Jurnal Inovasi Teknik Kimia*, 8(3), pp. 167–172, 2023. (in Indonesian)
<https://doi.org/10.31942/inteka.v8i3.8441>
- [12] Wulandari, Y. R., Chen, S. S., Hermosa, G. C., Hossain, M. S. A., Yamauchi, Y., Ahamad, T., Alshehri, S. M., Wu, K. C. W., Wu, H.-S. "Effect of N₂ flow rate on kinetic investigation of lignin pyrolysis", *Environmental Research*, 190, 109976, 2020.
<https://doi.org/10.1016/j.envres.2020.109976>
- [13] Abdullah, N., Safana, A. A., Sulaiman, F., Abdullahi, I. I. "A Comparative Analysis of Physical and Chemical Properties of Biochars and Bio-Oils Obtained from Pyrolytic Process of Mesocarp Fibre and Empty Fruit Bunch", *Solid State Phenomena*, 268, pp. 387–392, 2017.
<https://doi.org/10.4028/www.scientific.net/SSP.268.387>
- [14] Rezki, A. S., Wulandari, Y. R., Alvita, L. R., Sari, N. P. "Potensi Limbah Tandan Kosong Kelapa Sawit (TKKS) sebagai Bioenergi pada Produksi Bio-Oil dengan Metode Pirolisis: Efek Temperatur: Potential of Empty Fruit Bunches (EFB) Waste as Bioenergy to Produce Bio-Oil Using Pyrolysis Method: Temperature Effects", *Jurnal Rekayasa Bahan Alam Dan Energi Berkelanjutan*, 7(1), pp. 22–29, 2023.
<https://doi.org/10.21776/ub.rbaet.2023.007.01.04>
- [15] Wulandari, Y. R., Rezki, A. S., Afifah, D. A., Sari, N. P., Elsyana, V., Gustian, H. "Studi Karakteristik Komposisi Produk Katalitik Pirolisis TKKS dengan katalis Al White" (Study of Composition Characteristics of Catalytic Product Pyrolysis of TKKS with Al White catalyst), *JoASCE (Journal Applied of Science and Chemical Engineering)*, 1(1), pp. 22–26, 2023. (in Indonesian)
<https://doi.org/10.25181/joasce.v1i1.3020>
- [16] Slopiecka, K., Bartocci, P., Fantozzi, F. "Thermogravimetric analysis and kinetic study of poplar wood pyrolysis", *Applied Energy*, 97, pp. 491–497, 2012.
<https://doi.org/10.1016/j.apenergy.2011.12.056>
- [17] Arenas, C. N., Navarro, M. V., Martínez, J. D. "Pyrolysis kinetics of biomass wastes using isoconversional methods and the distributed activation energy model", *Bioresource Technology*, 288, 121485, 2019.
<https://doi.org/10.1016/j.biortech.2019.121485>
- [18] Sidek, F. N., Saleh, S., Abdul Samad, N. A. F. "Kinetic parameter estimation for pyrolysis of empty fruit bunch using model-fitting and model-free methods", *Materials Today: Proceedings*, 57, pp. 1241–1247, 2022.
<https://doi.org/10.1016/j.matpr.2021.11.141>
- [19] ASTM International "ASTM E986-97 Standard Practice for Scanning Electron Microscope Beam Size Characterization", ASTM International, West Conshohocken, PA, USA, 1997.
- [20] Dubdub, I., Al-Yaari, M. "Pyrolysis of Low Density Polyethylene: Kinetic Study Using TGA Data and ANN Prediction", *Polymers*, 12(4), 891, 2020.
<https://doi.org/10.3390/polym12040891>

- [21] Morin, M., Pécate, S., Masi, E., Hémati, M. "Kinetic study and modelling of char combustion in TGA in isothermal conditions", *Fuel*, 203, pp. 522–536, 2017.
<https://doi.org/10.1016/j.fuel.2017.04.134>
- [22] Yao, F., Wu, Q., Lei, Y., Guo, W., Xu, Y. "Thermal decomposition kinetics of natural fibers: Activation energy with dynamic thermogravimetric analysis", *Polymer Degradation and Stability*, 93(1), pp. 90–98, 2008.
<https://doi.org/10.1016/j.polyimdegradstab.2007.10.012>
- [23] Carrier, M., Auret, L., Bridgwater, A., Knoetze, J. H. "Using Apparent Activation Energy as a Reactivity Criterion for Biomass Pyrolysis", *Energy & Fuels*, 30(10), pp. 7834–7841, 2016.
<https://doi.org/10.1021/acs.energyfuels.6b00794>
- [24] The MathWorks, Inc. "MATLAB, (2016a)", [computer program] Available at: <https://www.mathworks.com/help/signal/ref/sgolayfilt.html> [Accessed: 04 March 2024]
- [25] Boakye, E. A. "Lignin Transformation and Characterization of Pyrolytic Products", PhD Dissertation, South Dakota State University, 2017.
- [26] Abdullah, C. I., Azzahari, A. D., Rahman, N. M. M. A., Hassan, A., Yahya, R. "Optimizing Treatment of Oil Palm-Empty Fruit Bunch (OP-EFB) Fiber: Chemical, Thermal and Physical Properties of Alkalized Fibers", *Fibers and Polymers*, 20(3), pp. 527–537, 2019.
<https://doi.org/10.1007/s12221-019-8492-0>
- [27] Iryani, D. A., Haryanto, A., Hidayat, W., Amrul, Talambanua, M., Hasanudin, U., Lee, S. "Torrefaction Upgrading Of Palm Oil Empty Fruit Bunches Biomass Pellets For Gasification Feedstock By Using Comb (*Counter Flow Multi-Baffle*) Reactor", In: 7th International Conference on Trends in Agricultural Engineering (TAE), Prague, Czech Republic, 2019, pp. 212–217. ISBN 978-80-213-2953-9
- [28] Elgharbawy, A. A., Alam, M. Z., Moniruzzaman, M., Kabbashi, N. A., Jamal, P. "Chemical and structural changes of pretreated empty fruit bunch (EFB) in ionic liquid-cellulase compatible system for fermentability to bioethanol", *3 Biotech*, 8(5), 236, 2018.
<https://doi.org/10.1007/s13205-018-1253-8>
- [29] Iskandar, W. M. E., Ong, H. R., Rahman Khan, M. M., Ramli, R. "Effect of ultrasonication on alkaline treatment of empty fruit bunch fibre: Fourier Transform Infrared Spectroscopy (FTIR) and morphology study", *Materials Today: Proceedings*, 66, pp. 2840–2843, 2022.
<https://doi.org/10.1016/j.matpr.2022.06.526>
- [30] Arshad, S. H. M., Ngadi, N., Wong, S., Amin, N. S., Razmi, F. A., Mohamed, N. B., Inuwa, I. M., Aziz, A. A. "Optimization of phenol adsorption onto biochar from oil palm empty fruit bunch (EFB)", *Malaysian Journal of Fundamental and Applied Sciences (MJFAS)*, 15(1), pp. 1–5, 2019.
<https://doi.org/10.11113/mjfas.v15n2019.1199>
- [31] Hamzah, N. S., Idris, S. S., Rahman, N. A., Abu Bakar, N. F., Matali, S. "Thermal Analysis of Co-Utilization of Empty Fruit Bunch and Silantek Coal Under Inert Atmosphere Using Thermogravimetric Analyzer (TGA)", *Frontiers in Energy Research*, 8, 608756, 2021.
<https://doi.org/10.3389/fenrg.2020.608756>
- [32] Wulandari, Y. R., Silmi, F. F., Rezki, A. S., Wu, H.-S., Sukma, V. A., Sudibyo, S. "TGA Study on Catalytic Thermal Degradation of Brown Solid (Fermented Product from Rice Straw) and Ash from Brown Solid as Catalyst", *CHEMICA: Jurnal Teknik Kimia*, 11(1), pp. 10–16, 2024.
<https://doi.org/10.26555/chemica.v11i1.221>
- [33] Siddiqi, H., Kumari, U., Biswas, S., Mishra, A., Meikap, B. C. "A synergistic study of reaction kinetics and heat transfer with multi-component modelling approach for the pyrolysis of biomass waste", *Energy*, 204, 117933, 2020.
<https://doi.org/10.1016/j.energy.2020.117933>
- [34] Cano-Pleite, E., Rubio-Rubio, M., Riedel, U., Soria-Verdugo, A. "Evaluation of the number of first-order reactions required to accurately model biomass pyrolysis", *Chemical Engineering Journal*, 408, 127291, 2021.
<https://doi.org/10.1016/j.cej.2020.127291>
- [35] Nyakuma, B. B., Wong, S., Oladokun, O. "Non-oxidative thermal decomposition of oil palm empty fruit bunch pellets: fuel characterisation, thermogravimetric, kinetic, and thermodynamic analyses", *Biomass Conversion and Biorefinery*, 11(4), pp. 1273–1292, 2021.
<https://doi.org/10.1007/s13399-019-00568-1>
- [36] Sukiran, M. A., Alaba, P. A., Nasrin, A. B., Aziz, A. A., Loh, S. K. "Thermal Analysis And Non-Isothermal Thermogravimetric Kinetics Analysis Using Coats-Redfern Method Of A Torrefied Empty Fruit Bunches", *Journal of Oil Palm Research (JOPR)*, 35(4), pp. 639–652, 2023.
<https://doi.org/10.21894/jopr.2023.0011>
- [37] Rama Rao, P., Ramakrishna, G. "Oil palm empty fruit bunch fiber: surface morphology, treatment, and suitability as reinforcement in cement composites- A state of the art review", *Cleaner Materials*, 6, 100144, 2022.
<https://doi.org/10.1016/j.clema.2022.100144>
- [38] Nadhari, W. N. A. W., Ishak, N. S., Danish, M., Atan, S., Mustapha, A., Karim, N. A., Hashim, R., Sulaiman, O., Yahaya, A. N. A. "Mechanical and physical properties of binderless particleboard made from oil palm empty fruit bunch (OPEFB) with addition of natural binder", *Materials Today: Proceedings*, 31, pp. 287–291, 2020.
<https://doi.org/10.1016/j.matpr.2020.06.009>
- [39] Mohamed, A. R., Awang, A. N., Salleh, N. H. M., Ahmad, R. "Thermal pyrolysis of empty fruit bunch (EFB) in a vertical fixed-bed reactor", *IOP Conference Series: Materials Science and Engineering*, 932, 012007, 2020.
<https://doi.org/10.1088/1757-899X/932/1/012007>
- [40] Ferreira, M. F. P., Oliveira, B. F. H., Pinheiro, W. B. S., Correa, N. F., França, L. F., Ribeiro, N. F. P. "Generation of biofuels by slow pyrolysis of palm empty fruit bunches: Optimization of process variables and characterization of physical-chemical products", *Biomass and Bioenergy*, 140, 105707, 2020.
<https://doi.org/10.1016/j.biombioe.2020.105707>

- [41] Novianti, S., Nurdiawati, A., Zaini, I. N., Prawisudha, P., Sumida, H., Yoshikawa, K. "Low-potassium Fuel Production from Empty Fruit Bunches by Hydrothermal Treatment Processing and Water Leaching", *Energy Procedia*, 75, pp. 584–589, 2015.
<https://doi.org/10.1016/j.egypro.2015.07.460>
- [42] Hardianto, T., Wenas, A. A., Juangsa, F. B. "Upgrading process of palm empty fruit bunches as alternative solid fuel: a review", *Clean Energy*, 7(6), pp. 1173–1188, 2023.
<https://doi.org/10.1093/ce/zkad059>
- [43] Puligundla, P., Oh, S.-E., Mok, C. "Microwave-assisted pretreatment technologies for the conversion of lignocellulosic biomass to sugars and ethanol: a review", *Carbon Letters*, 17(1), pp. 1–10, 2016.
<https://doi.org/10.5714/CL.2016.17.1.001>
- [44] Brodeur, G., Yau, E., Badal, K., Collier, J., Ramachandran, K. B., Ramakrishnan, S. "Chemical and Physicochemical Pretreatment of Lignocellulosic Biomass: A Review", *Enzyme Research*, 2011(1), 787532, 2011.
<https://doi.org/10.4061/2011/787532>
- [45] Wang, C., Lin, M., Yang, Q., Fu, C., Guo, Z. "The Principle of Steam Explosion Technology and Its Application in Food Processing By-Products", *Foods*, 12(17), 3307, 2023.
<https://doi.org/10.3390/foods12173307>